Pakistan J. Zool., vol. 57(6), pp 2521-2533, 2025 **DOI**: https://dx.doi.org/10.17582/journal.pjz/20250113172610

HLF: A Novel Epigenetically Regulated Tumor Suppressor and Diagnostic Biomarker in Breast Cancer

Kokab Farooq[1], Sheereen Gull[1], Zubia Farooq[2], Sitara Nisar[1], Sadia Bukhari[1] and Naveed Shahzad[1]*

[1]*School of Biological Sciences, University of the Punjab, Quaid-I-Azam Campus 54590, Lahore, Pakistan*
[2]*Shaukat Khanum Memorial Cancer Hospital and Research Centre, 54000 Lahore, Pakistan*

Article Information
Received 13 January 2025
Revised 25 February 2025
Accepted 13 March 2025
Available online 07 May 2025 (early access)
Published 19 September 2025

Authors' Contribution
KF collected the tissue samples, performed experimental work, analyzed data, and wrote the manuscript. SG contributed to data analysis. ZF performed histopathological analysis of the tissue samples. SN and SB contributed to the experimental work. NS supervised the whole project, secured funding, and reviewed, and finalized the manuscript. All authors contributed to the article and approved the submitted version.

Key words
***HLF*, Hypermethylation, Downregulation, Biomarker, Breast cancer, Tumor suppressor**

ABSTRACT

Breast cancer (BC) is a leading cause of cancer-related mortality in women. Early detection based on genetic and epigenetic biomarkers significantly improved the survival rates of BC. In this study, we investigated the epigenetic regulation and tumor suppressor role of a novel gene, hepatic leukaemia factor (*HLF*), in the development of BC and explored its potential use as a biomarker for BC diagnosis. Analysis of 50 paired breast tissue samples and two BC cell lines revealed significant downregulation of *HLF* in tumor tissues ($P<0.0001$) and cells compared to normal counterparts. Targeted CpG sites in the *HLF* promoter demonstrated hypermethylation in 70% of tumor samples (35/50). Whereas, 58% of tumor tissues exhibited concurrent hypermethylation and downregulation ($P=0.03$). *In-silico* analysis of samples from the TCGA-BRCA database also verified these findings. *In-vitro* demethylation assay confirmed the epigenetic silencing of *HLF*, as demethylation restored its expression in BC cells. Functional studies using ectopic expression of *HLF* in BC cell lines revealed tumour-suppressive properties, including reduced proliferation, invasiveness, migration, and enhanced DNA damage. This study convincingly identified *HLF* as a novel epigenetically silenced tumor suppressor gene and diagnostic biomarker in BC, providing preliminary evidence of its potential as a target for innovative diagnostic and therapeutic strategies for improving patient outcomes.

INTRODUCTION

Breast cancer (BC) is the most prevalent form of cancer globally, tragically claiming countless lives among women. Despite significant advancements in treatment including surgery, chemotherapy, and radiation, the prognosis and survival rates for BC patients remain meagre. Conventional diagnostic techniques, for instance, mammography, encounter limitations such as high costs, time consumption, and reduced efficacy in detecting small tumors (Ohuchi *et al*., 2016). While advanced imaging techniques like breast-specific gamma imaging (BSGI) and positron emission mammography (PEM) have emerged, early-stage diagnosis is still a challenge. Early detection significantly improves patient survival, with 5-year survival rates exceeding 90% for early-stage diagnoses but dropping to 25% for advanced cases (Thakur *et al*., 2022). Thus, there is a growing interest in discovering non-invasive biomarkers for early and accurate BC diagnosis. Epigenetic biomarkers, particularly tumor-specific DNA methylation alterations, have shown promise as they are stable, tissue-specific, detectable before cancer onset, and easily evaluated (Park, 2020; Vietri *et al*., 2021). DNA methylation patterns have been linked to the epigenetic silencing of tumor suppressor genes (TSGs) across various cancer types, including BC, offering the potential for early detection and prognosis assessment (Asci-Erkocyigit *et al*., 2023; Ayipo *et al*., 2022; Halabian *et al*., 2021).

One such gene is *HLF*; that belongs to the b/ZIP (basic region leucine zipper) transcription factors and member of the subfamily of PAR (proline and acidic amino acid-rich region). It is located on chromosome 17 at position 17q22 and involved in DNA binding and gene regulation through dimerization. Normally, *HLF* is expressed in hepatocytes as well as in liver-derived cell lines, with lower levels found in lungs, kidneys, and central nervous system

* Corresponding author: naveed.sbs@pu.edu.pk
0030-9923/2025/0006-2521 $ 9.00/00

neurons. It regulates circadian rhythms, hematopoiesis, and stress responses (Ahmadi *et al*., 2024; Hunger *et al*., 1992; Inaba *et al*., 1992). One prominent aspect of *HLF* involvement in cancer is its association with chromosomal translocations, particularly in leukaemia. This fusion gene (E2A-*HLF)* alters the apoptotic pathway and contributes to leukemogenesis by disrupting normal cellular processes and promoting uncontrolled cell proliferation (Chen *et al*., 2023). However, its role in cancer is paradoxical and tumour-specific, acting as either a TSG or oncogene (OG) depending on the cancer type. For instance, *HLF* exhibited tumor-suppressive properties in lung carcinoma (Chen *et al*., 2020), glioma (Chen *et al*., 2016; Liu *et al*., 2021) tongue tumors (Okano *et al*., 2023), cervical cancer (Liu *et al*., 2022), and prostate cancer (Zhou and Wang, 2023) where its downregulation was correlated with enhanced proliferation, metastasis, and therapy resistance. In contrast, it showed oncogenic behaviour in basal cell carcinoma (Waters *et al*., 2009), intrahepatic cholangiocarcinoma (Xiang *et al*., 2023), hepatocellular carcinomas (Musso and Beraza, 2019; Xiang *et al*., 2019), and Ovarian cancer (Han *et al*., 2023).

In BC, the role of *HLF* remains poorly understood. While some studies suggested that *HLF* enhances tumor progression, chemotherapy resistance, and ferroptosis resistance in triple-negative BC (TNBC) (Li *et al*., 2022), others described significant downregulation of *HLF* in breast tumors compared to normal tissues. Despite its documented inconsistent roles across cancers, the potential of *HLF* as an epigenetic biomarker in BC requires further investigation to clarify its clinical utility.

In this study, we analyzed transcriptional and epigenetic regulation of *HLF* in BC. We observed the anti-tumorigenic potential of *HLF* in BC cells and described it as a novel tumor suppressor gene silenced through hypermethylation in BC. Our findings propose *HLF* as a promising epigenetic biomarker for BC diagnosis and therapy, offering a potential avenue for improving patient outcomes.

MATERIALS AND METHODS

Patient samples and cell line processing

In this study, 100 breast tissue samples, comprising 50 malignant and 50 corresponding adjacent non-cancerous tissues, were analyzed. These samples were collected from patients at Sir Ganga Ram Hospital, Lahore, Pakistan (Bioethics Committee approval: Ref: Bioethics/094; 13/10/17), and were preserved in liquid nitrogen or in RNA later™ (Invitrogen) to maintain nucleic acid integrity. All relevant clinicopathological data and sample information were recorded and stored during the collection phase. DNA and RNA were extracted from the preserved samples for subsequent analyses by following the methodology described in (Gull *et al*., 2022; Naz *et al*., 2021).

Breast cancer cell lines (MCF-7, MDA-MB-231) representing two different molecular subtypes were obtained from the School of Biological Sciences (SBS), University of the Punjab, Lahore, Pakistan. Cells were cultured in Dulbecco's Modified Eagle Medium (DMEM) (Gibco, MD, USA) supplemented with 10% fetal bovine serum (FBS) and 1% penicillin-streptomycin and maintained at 37°C in a humidified atmosphere with 5% CO_2. Cell viability was assessed using Trypan blue staining, and viable cells were quantified with a Countess II automated cell counter (Thermo Fisher Scientific, USA). Standardized cell density (4×10^4 cells/cm^2) was maintained across all experimental setups to ensure consistency. Cell lines were cryopreserved in liquid nitrogen after serial passage for future assays.

HLF *expression analysis using qRT-PCR*

To analyze *HLF* expression change in BC cell lines and tumor tissues compared to corresponding normal tissues, qRT-PCR was performed. cDNA was synthesized from DNase-treated RNA using the RevertAid first strand cDNA synthesis kit (Thermo Scientific Cat. No. K1622), following the manufacturer's instructions. Gene expression was assessed using the SYBR Green Assay in the PicoReal SW 2.2 real-time PCR system (Thermo Fisher Scientific). Reactions were performed in 96-well plates, including non-template controls for quality assurance. Experiments were conducted in triplicate across two or three independent sets. PCR conditions included an initial denaturation at 95°C for 10 min, 35 cycles of 95°C for 30 sec, 58°C for 30 sec, and 72°C for 30 sec, followed by a final extension at 72°C for 5 min. *HLF* expression was normalized to β-actin and quantified using the 2^−ΔΔCt method (Livak and Schmittgen, 2001). Results are presented as relative fold changes in mRNA levels between tumor and normal samples. Primer sequences are listed in Table I.

Methylation-specific PCR (MSP) for HLF *promoter methylation analysis*

MSP was performed to assess differential methylation of CpG sites in the *HLF* promoter in BC cell lines and tumour tissues compared to normal tissues. The *HLF* promoter sequence was obtained from the eukaryotic promoter database (EPD) (https://epd.epfl.ch/) and analysed using MethPrimer Express v1.0 to predict CpG islands and design methylation-specific primers. Details of CpG islands in the promoter region of *HLF* are illustrated in Figure 1.

Table I. List of primer sequences used in this study.

Primer types	Forward primer (5'-3')	Amplicon size (bp)	*NCBI* gene accession number	Position	Exon F, R
qPCR Primers					
B-actin	F GATGAGATTGGCATGGCTTT R CACCTTCACCGTTCCAGTTT	100	NM_001101.5	chr7:5566779-5570232	4, 4
HLF	F ATCAGACCAGGTCAGCTGTT R TGGCTTCAGTTCTTCCTCAG	180	NM_002126	chr17:55264960-55325187	2-3, 3
MSP primers					
HLF methylation	F TTGTAAGGTTTTCGAAAATCGGC R AATAACGTCAAAACCCGCACC	137	NM_002126	Chr17: 552,648,25- 552,649,62	
HLF Unmethylation	F GTTGTAAGGTTTTTGAAAATTGGTG R AATAACATCAAAACCCACACCTC				

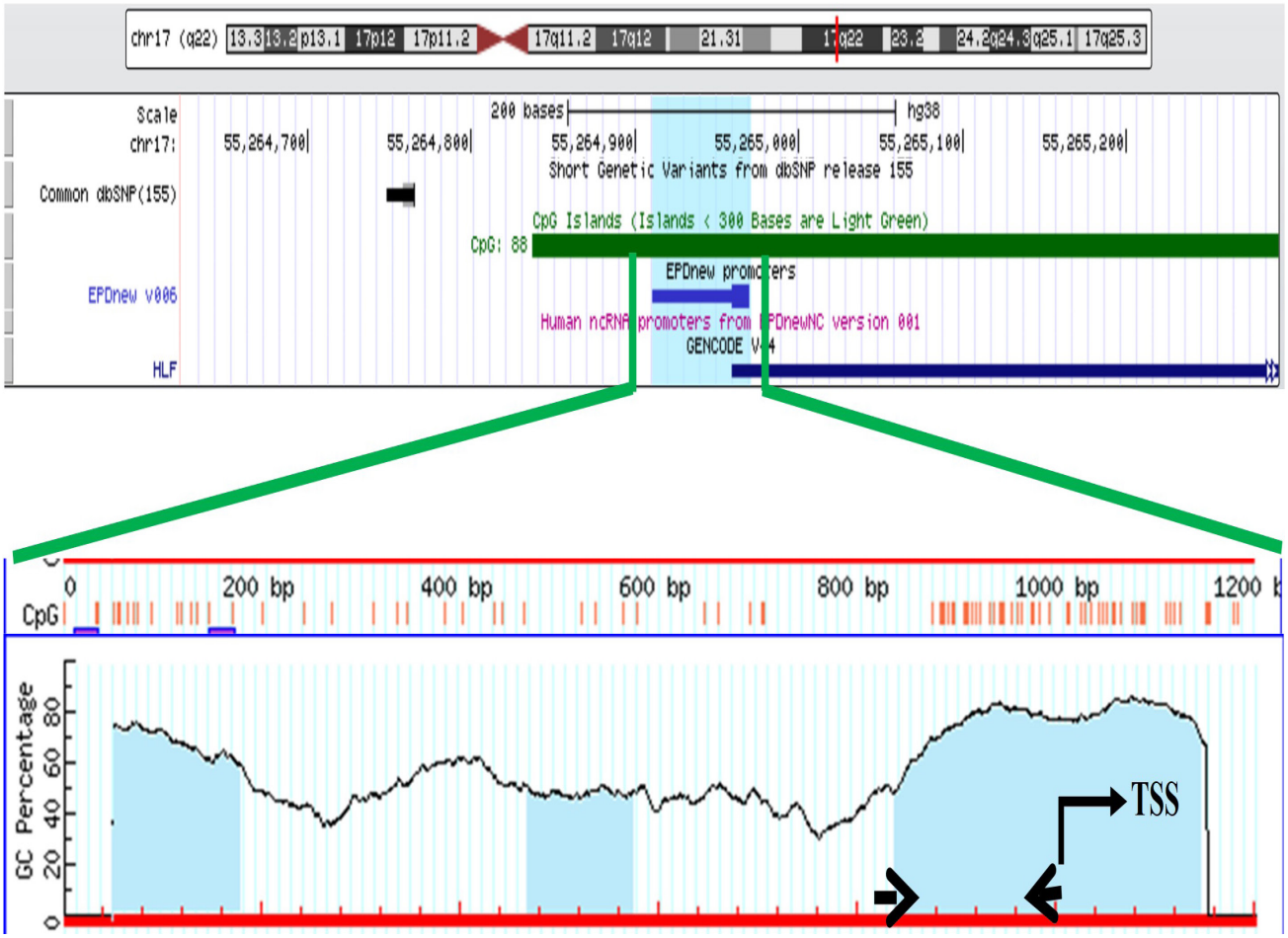

Fig. 1. *HLF* promoter region: *HLF is* located at a plus strand of Chr 17 (q22) indicated by the red bar on the chromosomal map. It has two promotors; we investigated the promotor corresponding to the transcript of interest Ref Seq: NM_002126._Sequence around the 1000 bp upstream of transcription start site (TSS) and 200bp downstream was obtained from UCSC on Human (GRCh38/hg38) Chr17: 552,639,59-552,651,59 position. Methprimer predicted three CpG islands within this sequence based on the following criteria: (Island size > 100, GC Percent > 50.0, Obs/Exp > 0.6). A large island containing TSS was investigated for methylation assay and the black arrow shows the primer location for MSP spanning the DNA from 552,648,25bp to 552,649,62 bp.

Table II. Data mining approach for the *in-silico* analysis of *HLF* expression and methylation from GDC (genomic data commons).

Data information	Expression analysis *in-silico*	Methylation analysis *in-silico*
Data portal	GDC	GDC
Primary tissue	Breast	Breast
Project	TCGA-BRCA	TCGA-BRCA
Data category	Transcriptome profiling	DNA Methylation
Data type	Gene expression quantification	Methylation beta Values
Experimental strategy	RNA-Seq (1095 cases)	Methylation Array (1097 cases)
Workflow type	STAR counts	SeSAMe Methylation Beta Estimation
Platform	----	- Illumina Human Methylation 450 (791 cases) - Illumina Human Methylation 27 (314 cases)

DNA from BC tissues and cell lines was treated with the EZ DNA Methylation-Gold™ Kit (Zymo Research, Cat. No. D5006) to achieve bisulfite conversion. Two primer sets were designed: "M" for methylated and "U" for unmethylated targeted CpG sites in bisulfite-converted DNA. Primer specificity was validated using commercially available methylated and unmethylated DNA controls (Zymo Research™). The MSP reaction mixture was prepared as described by Shahzad *et al*. (2020). The specificity of the primers was enhanced by using a touchdown PCR profile which included an initial denaturation at 95°C for 4 min, followed by 11 cycles of 94°C for 1 min, 67°C for 1 min (decreasing by 1°C per cycle), and 72°C for 1 min. This was followed by 35 cycles of 94°C for 30 sec, 57°C for 30 sec, and 72°C for 30 sec, with a final extension at 72°C for 5 min. PCR products were visualised on 2% agarose gels under UV light. The presence of amplified bands in the "M" or "U" reactions indicated the presence or absence of methylation at target CpG sites, respectively.

In-silico *expression and methylation analysis of* HLF

The expression and methylation differences of *HLF* between normal breast tissue and various subtypes of BC were also investigated through *in-silico* analysis. Data collection and analysis were performed following the methodology described by Shahzad *et al*. (2020). Briefly, primary data from the TCGA-BRCA project, sourced from GDC (Genomic Data Commons) provided transcriptomic and DNA methylation profiles for normal breast (NBr) tissues and BC subtypes, including invasive lobular carcinoma (ILBC), invasive ductal carcinoma (IDBC) and invasive basal carcinoma (IBC). Details about the data mining approach are outlined in Table II.

In-vitro *demethylation treatment*

An *in-vitro* demethylation assay was performed to examine whether reduced gene expression in BC cell lines is linked to promoter hypermethylation. MCF-7 and MDA-MB-231 cells were seeded in 6-well plates at a density of 1×10^6 cells/well and allowed to adhere for 24 h before treatment. The cells were then treated with 5-aza-2′-deoxycytidine (Aza) (Decitabine; Sigma, MO, USA) at 10 µM and 20 µM concentrations for four days. Culture media containing freshly prepared inhibitors were replaced every 24 h.

Following treatment, DNA and RNA were extracted from treated and untreated cells. The efficacy of demethylation was confirmed via MSP, while the impact on gene expression was evaluated using qRT-PCR. All experiments were performed in triplicate across two independent replicates.

Ectopic expression of HLF *and functional bioassays*

The effect of *HLF* overexpression in BC cell lines was analyzed by transfecting BC cells (MDA-MB-231 and MCF-7) with *HLF* expressing GFP labelled mammalian expression vector. For this purpose, an ORF clone of *HLF* "pcDNA3.1-C-eGFP-HLF" was obtained from GenScript Biotech, Singapore. Insertion of *HLF* ORF and its sequence accuracy was confirmed by digesting 500 ng of vector with HindIII and NotI (Fermentas) restriction enzymes for 1 h at 37℃. The map of the expression vector with *HLF* insert is shown in the Supplementary Figure 1.

BC cells were transfected with 2 µg of the expression vector (pcDNA3.1-C-eGFP-HLF) or empty vector (pcDNA3.1-C-eGFP) using Lipofectamine™ 3000 (Invitrogen) at 50% confluency. Non-transfected cells served as negative controls. Transfection success and efficiency were qualitatively assessed by fluorescent microscopy (IX83 Olympus) at regular intervals. The number of cells expressing green fluorescence was counted and calculated using the following formula:

$$\%Transfection\ efficiency = \frac{\text{Number of cells exhibiting GFP fluorescence}}{Total\ number\ of\ cells} \times 100$$

Quantitative assessment was performed by qRT-PCR using cell pellets collected at 0, 24, 48, and 72 h post-transfection.

The impact of *HLF* ectopic expression on cellular parameters (proliferation, colony formation, migration, and adhesion) and nuclear parameters (genotoxicity and apoptosis) was evaluated through various bioassays in transfected BC cells.

Cell proliferation assay

The effect of *HLF* overexpression on BC cell proliferation was assessed using a crystal violet assay. After a 72-h incubation post-transfection, media were removed, and cells were washed with 1X PBS to eliminate non-adherent cells. Cells were then fixed with 4% paraformaldehyde for 15 min at room temperature, followed by three PBS washes. Staining was performed with 0.1% crystal violet for 30 min at room temperature. Excess dye was removed, and the plates were air-dried before imaging at 10X magnification with a bright-field inverted microscope (TS Eclipse 100, Optika).

Colony formation assay

BC cells' survival and proliferative capacity transfected with an *HLF*-expression vector or empty vector were evaluated using a colony formation assay. After 72 h of transfection incubation, cells were trypsinized, counted, and seeded at 700 cells/well in 6-well plates. Following a 15-day incubation to assess clonogenic potential, cells were fixed with 4% paraformaldehyde and stained with 0.1% crystal violet. Distinct colonies were quantified under a light microscope, and images were captured at 4X magnification.

Invasion assay

The invasiveness of transfected cells was evaluated using transwell chambers (8 µm filters, SPL Insert™ cat#36124). At 72 h after post-HLF transfection, 1×10^5 nanoparticle cells were seeded into the upper chamber in a 100 µl serum-free medium. The lower chamber was filled with a medium containing 10% FBS as a chemoattractant. After 12 h of incubation at 37°C, the upper membrane was gently wiped with a cotton swab to remove non-invading cells and Matrigel coating. Invaded cells were fixed with 4% paraformaldehyde for 10 min, stained with 0.1% crystal violet for 5 min, and visualized under an inverted microscope at 10X magnification. Invaded cells were counted in four random fields per chamber, and the results were averaged across all experiments.

Wound healing assay

The horizontal migration and wound closure ability of transfected cells were assessed using a wound healing assay. BC cells were seeded at a density of 1×10^4 cells/cm² to reach 50% confluency after 24 h. A wound was created across the cell monolayer using a P-200 pipette tip, and detached cells were removed by gently washing with ice-cold 1X PBS. Wound closure was monitored and imaged at 0, 24, 48, and 72 h post-transfection using a bright-field microscope at 4X magnification. The distance of the wound closure was measured using ImageJ software (NIH, USA), and the rate of closure was calculated.

Hoechst 33342 staining

The nuclear morphology of transfected cells was observed by staining the cells after 72 h of transfection with fluorescent Hoechst 33342 stain (Thermo Scientific). Cells were fixed with 4% paraformaldehyde for 10 min, followed by three washes with 1X PBS (5 min each). A working solution of Hoechst 33342 stain was prepared by diluting a 10 mg/ml stock solution in 1X PBS at a 1:2,000 ratio. Cells were incubated with a sufficient working solution for 5 min at room temperature, allowing the dye to permeate and selectively stain nuclear DNA keeping protected from light. Morphological changes in apoptotic nuclei were visualized using a fluorescence microscope (excitation: 346 nm; emission: 460 nm). Images were captured at 20X and 40X magnification in four fields per well.

Flow cytometry

DNA damage in transfected cells was quantified via flow cytometry, following the protocol by Gull *et al.* (2022). Post-transfection, cells were trypsinized, washed twice with ice-cold 1X PBS, and pelleted at low speed. Cells were fixed in 70% ethanol at 4°C for 2 h, followed by additional washes to remove residual ethanol. Pellets were resuspended in 2 mL staining solution containing 50 µg/mL propidium iodide (PI) and 100 µg/mL RNase-A, and incubated at 37°C in the dark for 30 min. Samples were analyzed using a CyFlow Cube6 cytometer (Sysmex Partec) with FL2 channel gain set to 600 and background noise minimized by threshold adjustment. Data were processed using FCS Express V5 software, with results presented as DNA histograms. The Sub-G1 peak indicated apoptotic cells, while the G1 peak represented live cell populations.

Statistical analysis

All experiments were performed in triplicate and repeated independently three times unless otherwise stated. Statistical significance was set at $P < 0.05$, and results

were presented as mean ± SD or percentage. Data analysis was conducted using GraphPad Prism software (v. 5.0; GraphPad, San Diego, CA, USA). To assess differences between normal and tumor groups, as well as between transfected and non-transfected cells, a student's t-test was applied. The correlation between *HLF* methylation status and clinicopathological features of BC patients was evaluated using the Chi-square (χ^2) test.

RESULTS

HLF *expression is significantly reduced in BC tissues and cells*

The mRNA expression analysis of *HLF* in 50 paired breast tissue samples and two BC cell lines revealed significantly lower expression levels of *HLF* in the tumors and BC cell lines. Quantitative analysis showed a marked downregulation of *HLF* in MCF-7 (1.95±0.45) as well as in MDA-MB-231 (0.43±0.45) when compared to the mean expression of normal tissues (n=8, Mean 5.62±0.5) (Fig. 2A). Similarly, *HLF* expression was downregulated in breast tumors (Mean 2.4±1.3) relative to normal tissues (Mean 4.9±2.1), with a *P*-value<0.0001 (Fig. 2B).

In-silico analysis also supported our findings and demonstrated a significant downregulation of *HLF* in breast tumor tissues (ILBC: 13.8±1.8; IDBC: 14±1.7; IBC/others: 13.3±1.8) compared to normal breast tissues (NBr: 17.5±0.7) (Fig. 2C).

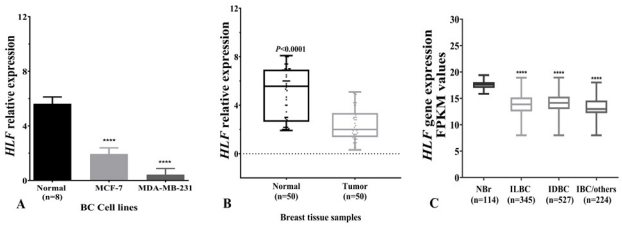

Fig. 2. *HLF* expression analysis: (A) Relative expression analysis of *HLF* in BC cell lines compared with the mean expression of 8 normal breast tissues. (B) Box-plot diagram of *HLF* gene expression in breast tumor (n=50) compared with adjacent normal tissue (n=50) samples. (C) *In-silico* analysis of *HLF* gene expression in normal and various subtypes of BC; NBr: Normal Breast Tissues, ILBC: Invasive Lobular Carcinoma, IDBC: Invasive Ductal Carcinoma, and IBC/others: Invasive Basal Carcinoma/less common BC subtypes. A two-tailed paired t-test indicates statistical significance. (*P<0.033, **P<0.002, ***P<0.001, ****P<0.0001).

HLF *promoter methylation is increased in BC tissues and cells*

MSP analysis using methylated and unmethylated DNA controls confirmed the specificity and accuracy of both the "M" and "U" *HLF* primer sets, with no evidence of cross-reactivity. In BC cell lines MCF-7 and MDA-MB-231, methylation analysis demonstrated significant hypermethylation of the targeted CpG sites within the *HLF* promoter, as amplification was observed as DNA band exclusively with the "M" primers (Fig. 3A).

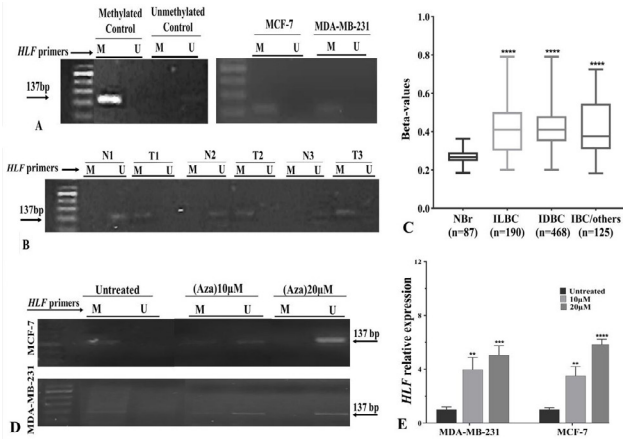

Fig. 3. *HLF* expression analysis: (A) MSP for *HLF* in two BC cell lines in comparison with methylated and unmethylated controls. (B) Representative MSP of *HLF* in breast tumors (T) and adjacent normal tissues (N) samples. (C) *In-silico* analysis of *HLF* methylation in breast normal and tumor tissues. NBr: Normal Breast Tissues, ILBC: Invasive Lobular Carcinoma, IDBC: Invasive Ductal Carcinoma, and IBC/others: Invasive Basal Carcinoma/less common BC subtypes. (D) Correlation between *HLF* gene expression and methylation levels in response to Aza treatment. A gradual reduction in *HLF* promoter methylation, demonstrating a concentration-dependent effect in MCF-7 and MDA-MB-231 and (E) corresponding increase in *HLF* expression. Two-tailed Mann-Whitney test *P*-values indicate statistical significance. (*P<0.033, **P<0.002, ***P<0.001, ****P<0.0001). Graphs show the mean of three technical repeats. S. D=Error bars.

Among the 50 paired BC tissue samples analyzed, the *HLF* promoter was hypermethylated in 35 (70%) BC tissues, as indicated by strong amplification with "M" primers. In contrast, normal tissues predominantly showed amplification with "U" primers in 40 (80%) samples, suggesting an absence of methylation. Partial or complete methylation was also observed in a few normal tissues, as evidenced by bands of varying intensities. Representative gel images of tissue samples are shown in Figure 3B. The difference in methylation levels between BC and normal tissues was statistically significant (P= 0.003).

Additionally, *in-silico* analysis of *HLF* methylation levels (beta-value) confirmed the statistically significant

increase in methylation among various BC subtypes (ILBC: 0.42±0.14; IDBC: 0.42±0.12; IBC/others: 0.43±0.16) compared to normal breast tissues (0.27±0.03). However, there were no noticeable methylation differences for *HLF* between the tumor subtypes (Fig. 3C).

5-aza-2'-deoxycytidine (Aza) treatment decreased HLF *methylation and restored its expression in BC cell lines*

The Aza-mediated demethylation treatment led to a significant reduction in the methylation levels of the *HLF* promoter, as confirmed by MSP analysis. Correspondingly, a marked increase in *HLF* gene expression was observed in both cell lines compared to the untreated controls. The expression levels exhibited a proportional increase correlating with a gradual reduction in methylation, demonstrating a clear relationship between Aza treatment concentration and *HLF* expression. However, *HLF* methylation was more pronounced in MCF-7 compared to MDA-MB-23, (Fig. 3D, E).

Clinicopathological characteristics of BC Samples and their association with HLF *methylation*

Histological features of various BC subtypes including non-ductal and ductal BC tissues are presented in Supplementary Figure 2. Most of the samples used in this study were from patients over 50 years old and were in the postmenopausal stage. Tumors were primarily larger than 20 mm, with a significant proportion classified as ductal carcinoma. While nodal involvement was observed in some cases, the majority lacked signs of metastasis. According to TNM staging, most cases were categorised as stage I or II, representing early-stage BC. The association of *HLF* methylation with clinicopathological parameters is summarized in Table III. There was no significant association between *HLF* aberrant promoter methylation and clinical features of BC samples. Of the 50 BC cases analysed, 35 (70%) exhibited *HLF* hypermethylation. Methylation was predominantly observed in early-stage cases, with 23 out of 30 TNM stage I/II samples (77%) showing hypermethylation. Similarly, out of 37 cases with no metastasis 27 cases showed hypermethylation (73%). There were 35 cases without nodal involvement; among them, 25 showed hypermethylation (72%). Among the 48 ductal carcinoma cases, 33 (69%) exhibited *HLF* hypermethylation. These findings suggest a trend toward hypermethylation in early-stage and non-metastatic BC cases, although the associations were not statistically significant.

Ectopic expression of HLF *in BC cells*

The role of *HLF* in tumor development was investigated by ectopically expressing the open reading frame (ORF) of *HLF* in MCF-7 and MDA-MB-231 cell lines. Before transfection, restriction digestion of the expression vector confirmed the cloning of *HLF* into the pcDNA3.1-C-eGFP vector (Fig. 4A). Peak transfection efficiency was observed at 72 h where MCF-7 and MDA-MB-231 cells exhibited transfection rates of 60% and 80%, respectively (Fig. 4B). Furthermore, RT-PCR confirmed the overexpression of *HLF* in transfected cells, showing a progressive increase in mRNA levels over time, with a maximum of 72 h (Fig. 4C). Based on these findings, all subsequent functional assays were conducted at the 72-h mark, ensuring optimal transfection efficiency and *HLF* overexpression.

Table III. Association between *HLF* promoter methylation and mRNA expression with clinicopathological features of the BC samples.

Characteristics	Cases n=50	*HLF* promoter methylation		*p value
		Present n=35	Absent n=15	
Age at diagnosis				
≥ 50	47 (94%)	32 (68%)	15 (32%)	0.2
<50	03 (6%)	03 (100%)	0 (%)	
Menopausal status				
Pre	0 (nil)	0 (nil%)	0 (nil%)	nil
Post	50 (100%)	35 (70%)	15 (30%)	
Tumor size				
≤20 mm	11 (22%)	8 (73%)	3 (27%)	0.8
>20 mm	39 (78%)	27 (70%)	12 (30%)	
Histological type				
Non ductal	2 (4%)	2 (100%)	0 (nil%)	0.3
Ductal	48 (96%)	33 (69%)	15 (31%)	
Nodal involvement				
Negative	35 (70%)	25 (72%)	10 (28%)	0.7
Positive	15 (30%)	10 (67%)	5 (33%)	
Metastasis				
Yes	13 (26%)	8 (62%)	5.(38%)	0.4
No	37 (74%)	27 (73%)	10 (27%)	
TNM stage				
Early I/II	30 (60%)	23 (77%)	07 (23%)	0.2
Advance III/IV	20 (40%)	12 (60%)	08 (40%)	

Data are reported as frequencies and percentages. Differences between proportions were assessed by *Chi square test. Significant at $P<0.0$

HLF *overexpression suppressed tumorigenic and metastatic properties of BC cells*

Functional bioassays for *HLF*-expressing transfected

BC cells revealed a significant reduction in their tumorigenic properties. Induced expression of *HLF* markedly inhibited cell proliferation, reducing growth rates by 79% in MCF-7 cells and 90% in MDA-MB-231 cells compared to controls transfected with the empty vector (pcDNA3.1-C-eGFP) (Fig. 5A). Similarly, induced expression of *HLF* also affected the clonogenic potential of BC cells, significantly reducing both colony size and number. *HLF* expressing MCF-7 and MDA-MB-231 cells formed an average of 100±8 and 150±5 colonies respectively, compared to 700±7 and 800±4 colonies formed by empty vector-transfected cells. The ectopic expression of *HLF* markedly diminished cell survival ability by 70% in MCF-7 cells and 85% in MDA-MB-231 cells (Fig. 5B).

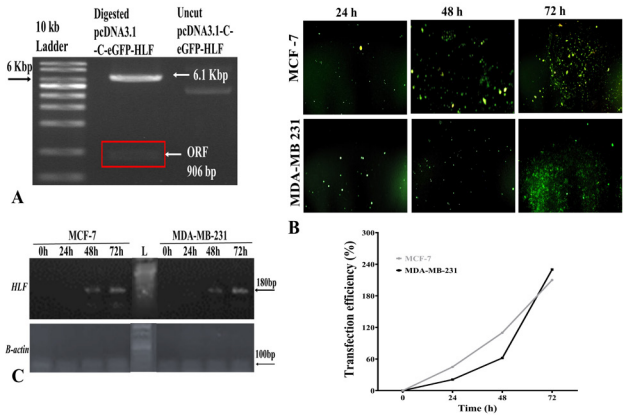

Fig. 4. *HLF* transfection efficacy and its confirmation: (A) Digestion of pcDNA3.1-C-eGFP-HLF with HindIII and Not1 restriction enzymes confirmed the presence of *HLF* insert as indicated by the red box. (B) (Upper panel) Qualitative assessment of transfection efficiency by GFP labelled vector for *HLF* overexpression. (Lower panel) Percentage transfection efficiency at various time points. (C): Representative gel images of qRT-PCR for quantitative assessment of *HLF* transfection. The expression of β-actin remained unchanged throughout the transfection period.

HLF overexpression also suppressed BC cells metastatic potential. Transwell invasion assays revealed a significant reduction in invasiveness, with invasion rates decreasing to 20% in MCF-7 and 34% in MDA-MB-231 cells compared to controls (Fig. 6A). Wound healing assays showed a striking inhibition of migratory capacity, with wound closure rates reduced to 3.5% in MCF-7 and 7% in MDA-MB-231 cells, compared to 46.1% and 85.7%, respectively, in empty vector-transfected cells (Fig. 6B).

HLF *overexpression-induced apoptosis via DNA damage*

The ectopic expression of *HLF* promoted apoptosis in BC cells, primarily through the induction of DNA damage. Hoechst staining revealed nuclear fragmentation and bright blue hyperchromatic nuclei, hallmark features of DNA damage, in *HLF*-transfected cells (Fig. 7A). Flow cytometric analysis further validated these findings, demonstrating a pronounced increase in apoptotic cell populations and a decrease in viable cells. Cells overexpressing *HLF* showed growth arrest in the G1 phase, as reflected by an elevated G1 peak, while control cells transfected with the empty vector displayed a higher count of live cells and a reduced sub-G1 apoptotic fraction (Fig. 7B).

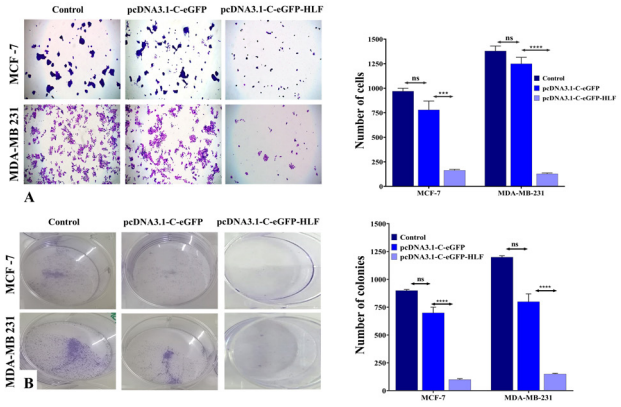

Fig. 5. (A) Proliferation assay for *HLF*: (left) Post-transfection images of the crystal violet assay represented a reduction in proliferation in both cell lines (10X magnification). (right) graphical representation of no. of cells counted after staining with crystal violet. (B) Colony formation assay for *HLF*: (left) Induced *HLF* expression significantly reduced the colony formation potential of BC cells. The appearance of discrete and distinguishable colonies was captured after 2 weeks of post-transfection seeding of the cells. (magnification 4X). (right) Graphical representation of no. of colonies counted after staining with crystal violet. A two-tailed t-test indicates statistical significance between the cells transfected with empty vector control (pcDNA3.1-C-eGFP) and HLF-expressing vector (pcDNA3.1-C-eGFP-HLF). The difference between non-transfected cells and cells transfected with empty vector control is not significant (ns). S. D=Error bars.

Collectively, these results provide compelling evidence that *HLF* suppresses tumorigenic and metastatic properties in BC cells by impairing proliferation, inhibiting migration and invasion, and inducing apoptosis through DNA damage.

DISCUSSION

Early and accurate diagnosis of BC is crucial

in improving survival rates, yet identifying reliable biomarkers remains a challenge. Our study aimed to identify novel epigenetically regulated tumor suppressor genes that could serve as potential diagnostic markers. We focused on genes exhibiting concurrent downregulated expression and hypermethylation in BC by analysing transcriptomic and methylation microarrays. Among the candidates, gene encoding *HLF*, PAR bZIP transcription factor emerged as a prominent candidate with a potential positive diagnostic indicator of BC. Upon experimental verification, our findings suggested that *HLF* is epigenetically inactivated in BC, contributing to tumorigenesis and may be of relevance to the initiation, maintenance or progression of cancers of the female breast.

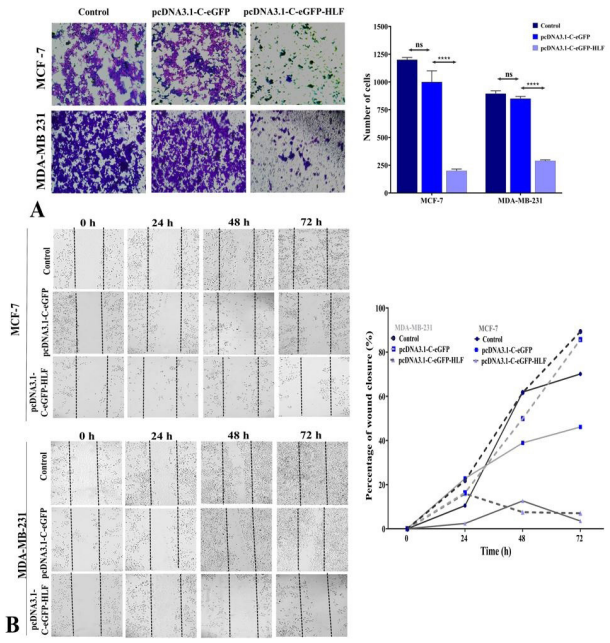

Fig. 6. (A) Invasion assay for *HLF*: (left) Representative images of Transwell invasion assay in non-transfected control and cells transfected with empty vector and HLF-vector. (10X magnification). (right) Graphical representation of the no. of cells that passed through the membrane after transfection. MDA-MB-231 displayed more invasiveness than MCF-7. Two-tailed t-test indicates statistical significance between the cells transfected with empty vector control (pcDNA3.1-C-eGFP) and HLF-expressing vector (pcDNA3.1-C-eGFP-HLF). The difference between non-transfected cells and cells transfected with empty vector control is not significant (ns). S. D=Error bars. (B) Wound healing assay for *HLF*: Post-transfection images of transfected BC cells with pcDNA3.1-C-eGFP and pcDNA3.1-C-eGFP-HLF, while non-transfected cells serve as a control, illustrating cell motility and wound healing at various time points. (magnification 4X). Percentage of wound healing in BC cells relative to controls at 0, 24, 48, and 72 h.

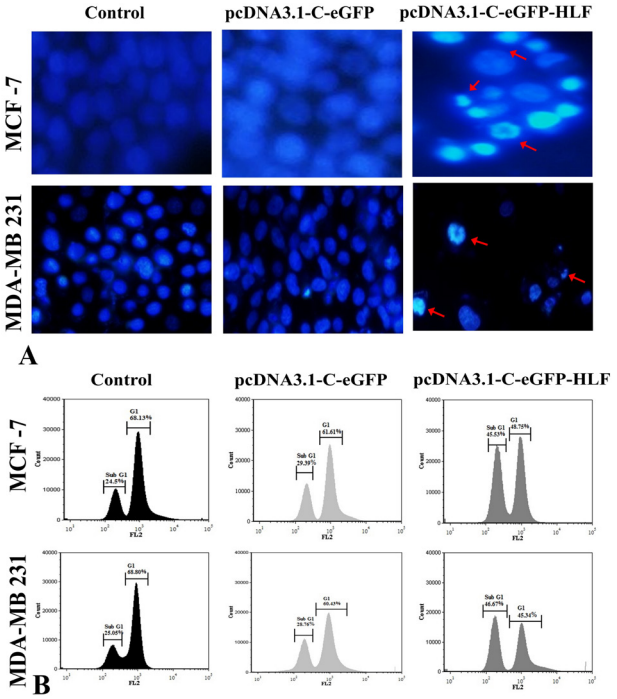

Fig. 7. (A) Hoechst staining for *HLF*: Morphological changes visualized by fluorescence microscopy after staining. Nuclear thickening and nuclear fragmentation increased significantly with time in *HLF* overexpressing cells indicated by the red arrow. (magnification 40X). (B) Flow cytometry for *HLF*: Representative data from one of the three experiments of PI staining followed by flow cytometry. Abundant apoptosis (Sub-G1 peak) and decreased no. of the live cell population (G1 peak) is observable in *HLF* overexpressing cells.

Our study revealed significantly decreased expression of *HLF* not only in BC tissues and cell lines during experimental analysis but also through *in-silico* analysis of external datasets, which consistently revealed reduced *HLF* expression in various histological subtypes of BC (IBC, ILBC, and IDBC) compared to normal breast samples (Fig. 2). Recent studies have also confirmed that *HLF* was downregulated in BC compared to normal tissues and has tumour-suppressive properties (Li *et al*., 2024; Mamoor, 2021; Vivarelli *et al*., 2024). Intriguingly, in a Chinese study, it was observed that increased *HLF* expression in TNBC is associated with chemotherapy resistance and ferroptosis, indicating a potential oncogenic role (Li *et al*., 2022, 2023). However, these conclusions were primarily drawn from bioinformatics analyses of TCGA and GEO datasets without experimental validation in clinical samples, leaving their findings open to question.

To address these discrepancies and reaffirm the reduced expression of *HLF* in BC, we performed an additional expression analysis using UALCAN. These results further validated our findings, demonstrating decreased *HLF* expression across BC subtypes, including luminal, HER2-positive, and TNBC (Supplementary Fig. 2). This comprehensive analysis not only strengthens our findings but also provides a robust counterpoint to the conclusions of Li *et al*. (2023), reaffirming the tumor-suppressive role of *HLF* in BC.

Our findings further revealed that *HLF* silencing in BC is primarily driven by promoter hypermethylation, a mechanism previously unexplored in BC. Methylation analysis focusing on the CpG target sites within the *HLF* promoter revealed significant hypermethylation (P=0.003) in 70% of the BC tissue samples and both BC cell lines. This observation was also supported by *in-silico* analysis and significant *HLF* hypermethylation was observed in various BC subtypes (Fig. 3).

DNA methylation has been described to regulate the *HLF* expression in various cancers and reduces its expression by affecting the binding of RNA polymerase II to its promoter (Chen *et al*., 2020; Gao *et al*., 2010; Takeshima *et al*., 2009). To further investigate the functional impact of DNA methylation on *HLF* expression, BC cell lines were treated with the demethylating agent AZA to induce gene reactivation through DNA demethylation (Khamas *et al*., 2012; Seelan *et al*., 2018; Shahzad *et al*., 2020). Treatment with Aza effectively reversed promoter methylation and significantly restored *HLF* expression, emphasizing the regulatory role of DNA methylation in its silencing (Fig. 3D, E). Interestingly, our study observed that the majority of BC tissues that exhibited downregulated *HLF* expression also displayed promoter hypermethylation in at least 58% of the BC samples making this correlation significant. However, a fraction of the samples still displayed *HLF* downregulation without a corresponding increase in promoter methylation suggesting the involvement of additional genetic factors in the silencing of *HLF* such as genetic deletion (Chen *et al*., 2016, 2020; Han *et al*., 2023).

We further explored the relationship between *HLF* promoter methylation and the clinicopathological characteristics of BC patients. We observed no statistically significant associations, likely due to the limited sample size. However, *HLF* hypermethylation was more prevalent in early-stage BC (stages I/II) without metastasis or lymph node involvement. This suggests that *HLF* promoter hypermethylation may contribute to early BC development, particularly in ductal carcinoma, where it was present in 69% of cases. These findings suggest the potential of *HLF* hypermethylation as an indicator for early BC diagnosis, which requires validation in larger cohorts with detailed clinical data.

Finally, we investigated the functional role of *HLF* in BC cells and identified its tumor-suppressive properties. Ectopic expression of *HLF* led to the significant inhibition of BC cell proliferation, migration, stemness, and invasiveness (Figs. 5, 6). Additionally, *HLF* reactivation led to significant DNA damage, cell cycle disruption, and increased apoptosis, highlighting its critical involvement in modulating key cancer-related pathways (Fig. 7). Similar tumour suppressive roles of *HLF* have also been reported in glioma, lung carcinoma, and cervical cancer, where *HLF* acts as a tumor suppressor by regulating pathways like miR-132/TTK, NF-κB, and Hippo signalling (Chen *et al*., 2016, 2020; Han *et al*., 2023). These observations imply that HLF is a potential universal biomarker and a promising therapeutic target. Although the exact mechanisms through which *HLF* exerts its anti-tumor effects in BC remain undefined, its involvement in other cancers suggests that similar mechanisms may be involved.

Despite its oncogenic roles in some cancers, such as basal cell carcinoma and ovarian cancer (Han *et al*., 2023; Waters *et al*., 2009), our results emphasise its context-dependent behavior, firmly establishing its tumor-suppressive role in BC. This dual nature of transcription factors is a common phenomenon that reflects the complex interplay of signaling networks specific to different tissue and tumor microenvironments (Hunger *et al*., 1992; Shen *et al*., 2018). This study addresses key gaps in BC research by providing robust experimental evidence of *HLF* silencing via promoter hypermethylation and demonstrating its tumor-suppressive properties. These findings not only establish *HLF* as a novel epigenetic biomarker for BC but also offer a potential avenue for therapeutic intervention. Future studies should investigate additional epigenetic regulators, such as intragenic methylation and chromatin remodeling, to further elucidate the mechanisms governing *HLF* silencing. Expanding these insights could lead to the development of comprehensive biomarker panels for BC, advancing early detection and personalized treatment strategies.

CONCLUSION

This study proposed *HLF* as a novel tumor suppressor gene epigenetically silenced in breast BC through promoter hypermethylation. Our findings further demonstrated that *HLF* ectopic expression contributes to tumor suppression by reducing cell proliferation, migration, and invasiveness while increasing apoptosis. These findings established *HLF* as an important player in BC pathogenesis and paved

the way for its development as a clinical biomarker for early detection and targeted therapies.

DECLARATIONS

Acknowledgements

We extend our thanks to the School of Biological Sciences (SBS) at Punjab University, Lahore. Pakistan, for providing the necessary research facilities and infrastructure to carry out this study.

Funding

We express gratitude to the Higher Education Commission (HEC) of Pakistan for funding this research through the National Research Program for Universities (NRPU) (Project 8461/Punjab/NRPU/RandD/HEC/2017).

IRB approval

This study was approved by the Institutional Bioethics Committee (Bioethics/094;13-10-17) of University of the Punjab, Lahore, Pakistan.

Ethical statement

Informed consent was obtained from all participants involved in the study.

Data availability statement

All data generated or analyzed during this study are included in this article (and its Supplementary Information files), further inquiries can be directed to the corresponding author.

Supplementary material

There is supplementary material associated with this article. Access the material online at: https://dx.doi.org/10.17582/journal.pjz/20250113172610

Statement of conflicts of interest

The authors have declared no conflict of interest.

REFERENCES

Ahmadi, M., Mohajeri, K.A., Morshedzadeh, F., Saffarzadeh, N., Ghaderian, S.M.H., Ghafouri-Fard, S. and Mousavi, P., 2024. *HLF* is a promising prognostic, immunological, and therapeutic biomarker in human tumors. *Biochem. Biophys. Rep*., **38**: 101725. https://doi.org/10.1016/j.bbrep.2024.101725

Asci-Erkocyigit, B., Ozufuklar, O., Yardim, A., Guler Celik, E. and Timur, S., 2023. Biomarker detection in early diagnosis of cancer: Recent achievements in point-of-care devices based on paper microfluidics. *Biosensors*, **13**: 387. https://doi.org/10.3390/bios13030387

Ayipo, Y.O., Ajiboye, A.T., Osunniran, W.A., Jimoh, A.A. and Mordi, M.N., 2022. Epigenetic oncogenesis, biomarkers and emerging chemotherapeutics for breast cancer. *Biochim. Biophys. Acta BBA Gene Regul. Mech*., **1865**: 194873. https://doi.org/10.1016/j.bbagrm.2022.194873

Chen, J., Liu, A., Lin, Z., Wang, B., Chai, X., Chen, S., Lu, W., Zheng, M., Cao, T., Zhong, M., Li, R., Wu, M., Lu, Z., Pang, W., Huang, W., Xiao, L., Lin, D., Wang, Z., Lei, F., Chen, X., Long, W., Zheng, Y., Chen, Q., Zeng, J., Ren, D., Li, J., Zhang, X. and Huang, Y., 2020. Downregulation of the circadian rhythm regulator HLF promotes multiple-organ distant metastases in non-small cell lung cancer through PPAR/NF-κb signaling. *Cancer Lett*., **482** : 56–71. https://doi.org/10.1016/j.canlet.2020.04.007

Chen, S., Li, Y., Wang, Z., Feng, L., Jia, Y., Mo, X., Wang, Y., Jiang, Q., Huang, X. and Lai, Y., 2023. Improved outcomes in E2A: HLF positive B-cell acute lymphoblastic leukemia by chimeric antigen receptor T cell therapy and BCL-2 inhibitor. *Chin. Med. J.* (Engl.), **136**: 1382–1384. https://doi.org/10.1097/CM9.0000000000002481

Chen, S., Wang, Y., Ni, C., Meng, G. and Sheng, X., 2016. HLF/miR-132/TTK axis regulates cell proliferation, metastasis and radiosensitivity of glioma cells. *Biomed. Pharmacother*., **83**: 898–904. https://doi.org/10.1016/j.biopha.2016.08.004

Gao, Z., Liu, H.L., Daxinger, L., Pontes, O., He, X., Qian, W., Lin, H., Xie, M., Lorkovic, Z.J., Zhang, S., Miki, D., Zhan, X., Pontier, D., Lagrange, T., Jin, H., Matzke, A.J.M., Matzke, M., Pikaard, C.S. and Zhu, J.K., 2010. An RNA polymerase II- and AGO4-associated protein acts in RNA-directed DNA methylation. *Nature*, **465**: 106–109. https://doi.org/10.1038/nature09025

Gull, S., Farooq, K., Tayyeb, A., Imran Arshad, M. and Shahzad, N., 2022. Ethanolic extracts of Pakistani euphorbiaceous plants induce apoptosis in breast cancer cells through induction of DNA damage and caspase-dependent pathway. *Gene*, **824**: 146401. https://doi.org/10.1016/j.gene.2022.146401

Halabian, R., Valizadeh, A., Ahmadi, A., Saeedi, P., Azimzadeh, J.S. and Alivand, M.R., 2021. Laboratory methods to decipher epigenetic signatures: A comparative review. *Cell. mol. Biol. Lett*., **26**: 46. https://doi.org/10.1186/s11658-021-00290-9

Han, T., Chen, T., Chen, L., Li, K., Xiang, D., Dou, L., Li, H. and Gu, Y., 2023. HLF promotes ovarian cancer progression and chemoresistance via regulating Hippo signaling pathway. *Cell Death Dis*., **14**: 1–13. https://doi.org/10.1038/s41419-023-06076-5

Hunger, S.P., Ohyashiki, K., Toyama, K. and Cleary, M.L., 1992. Hlf, a novel hepatic bZIP protein, shows altered DNA-binding properties following fusion to E2A in t(17;19) acute lymphoblastic leukemia. *Genes Dev*., **6**: 1608–1620. https://doi.org/10.1101/gad.6.9.1608

Inaba, T., Roberts, W.M., Shapiro, L.H., Jolly, K.W., Raimondi, S.C., Smith, S.D. and Look, A.T., 1992. Fusion of the leucine zipper gene HLF to the E2A gene in human acute b-lineage leukemia. *Science*, **257**: 531–534. https://doi.org/10.1126/science.1386162

Khamas, A., Ishikawa, T., Shimokawa, K., Mogushi, K., Iida, S., Ishiguro, M., Mizushima, H., Tanaka, H., Uetake, H. and Sugihara, K., 2012. Screening for epigenetically masked genes in colorectal cancer using 5-Aza-2'-deoxycytidine, microarray and gene expression profile. *Cancer Genom. Proteom*., **9**: 67–75.

Li, H., Yang, P., Wang, J., Zhang, J., Ma, Q., Jiang, Y., Wu, Y., Han, T. and Xiang, D., 2022. HLF regulates ferroptosis, development and chemoresistance of triple-negative breast cancer by activating tumor cell-macrophage crosstalk. *J. Hematol. Oncol. J. Hematol. Oncol*., **15**: 2. https://doi.org/10.1186/s13045-021-01223-x

Li, J., He, D., Li, S., Xiao, J. and Zhu, Z., 2023. Ferroptosis: The emerging player in remodeling triple-negative breast cancer. *Front. Immunol*., **14**. https://doi.org/10.3389/fimmu.2023.1284057

Li, S.Y., Hammarlund, J.A., Wu, G., Lian, J.W., Howell, S.J., Clarke, R.B., Adamson, A.D., Gonçalves, C.F., Hogenesch, J.B., Anafi, R.C. and Meng, Q.J., 2024. Tumor circadian clock strength influences metastatic potential and predicts patient prognosis in luminal A breast cancer. *Proc. natl. Acad. Sci*., **121**: e2311854121. https://doi.org/10.1073/pnas.2311854121

Liu, H., Xie, H., Zhao, Y., Zhang, W. and Zhang, Y., 2021. DNA methylation-mediated down-regulation of TMEM130 promotes cell migration in breast cancer. *Acta Histochem*., **123**: 151814. https://doi.org/10.1016/j.acthis.2021.151814

Liu, W., Jiang, Q., Sun, C., Liu, S., Zhao, Z. and Wu, D., 2022. Developing a 5-gene prognostic signature for cervical cancer by integrating mRNA and copy number variations. *BMC Cancer*, **22**: 192. https://doi.org/10.1186/s12885-022-09291-z

Livak, K.J. and Schmittgen, T.D., 2001. Analysis of relative gene expression data using real-time quantitative PCR and the 2(-Delta Delta C(T)) method. *Methods San Diego Calif*., **25**: 402–408. https://doi.org/10.1006/meth.2001.1262

Mamoor, S., 2021. *Differential expression of betaine-homocysteine S-methyltransferase 2 in cancers of the breast.* https://doi.org/10.31219/osf.io/ac3v2

Musso, O. and Beraza, N., 2019. Hepatocellular carcinomas: Evolution to sorafenib resistance through hepatic leukaemia factor. *Gut*, **68**: 1728–1730. https://doi.org/10.1136/gutjnl-2019-318999

Naz, H., Gull, S., Bashir, Q., Rashid, N. and Shahzad, N., 2021. Thermococcus kodakarensis-derived L-asparaginase: A candidate for the treatment of glioblastoma. *Biologia* (Bratisl.) **76**: 1305–1314. https://doi.org/10.2478/s11756-021-00678-0

Ohuchi, N., Suzuki, A., Sobue, T., Kawai, M., Yamamoto, S., Zheng, Y.-F., Shiono, Y.N., Saito, H., Kuriyama, S., Tohno, E., Endo, T., Fukao, A., Tsuji, I., Yamaguchi, T., Ohashi, Y., Fukuda, M. and Ishida, T., 2016. Sensitivity and specificity of mammography and adjunctive ultrasonography to screen for breast cancer in the Japan Strategic Anti-cancer Randomized Trial (J-START): A randomised controlled trial. *Lancet*, **387**: 341–348. https://doi.org/10.1016/S0140-6736(15)00774-6

Okano, L.M., Fonseca, L.M.M. da, Erthal, I.D. and Malta, T.M., 2023. Epigenomic integrative analysis pinpoint master regulator transcription factors associated with tumorigenesis in squamous cell carcinoma of oral tongue. *Genet. mol. Biol.*, **46**: e20220358. https://doi.org/10.1590/1678-4685-gmb-2022-0358

Park, H.L., 2020. Epigenetic biomarkers for environmental exposures and personalized breast cancer prevention. *Int. J. Environ. Res. Publ. Hlth*., **17**: 1181. https://doi.org/10.3390/ijerph17041181

Seelan, R.S., Mukhopadhyay, P., Pisano, M.M. and Greene, R.M., 2018. Effects of 5-Aza-2′-deoxycytidine (decitabine) on gene expression. *Drug Metab. Rev*., **50**: 193–207. https://doi.org/10.1080/03602532.2018.1437446

Shahzad, N., Munir, T., Javed, M., Tasneem, F., Aslam, B., Ali, M., Mutahir, Z., Akhtar Ali, M., Umer, M., Ahmad, M., Farooq, K., Hassan, U., Mustafa, T., Anjum, R.S. and Shakoori, A.R., 2020. SHISA3, an antagonist of the Wnt/β-catenin signaling, is epigenetically silenced and its ectopic expression suppresses growth in breast cancer. *PLoS One*,

15: e0236192. https://doi.org/10.1371/journal.pone.0236192

Shen, L., Shi, Q. and Wang, W., 2018. Double agents: Genes with both oncogenic and tumor-suppressor functions. *Oncogenesis*, **7**: 1–14. https://doi.org/10.1038/s41389-018-0034-x

Takeshima, H., Yamashita, S., Shimazu, T., Niwa, T. and Ushijima, T., 2009. The presence of RNA polymerase II, active or stalled, predicts epigenetic fate of promoter CpG islands. *Genome Res*., **19**: 1974–1982. https://doi.org/10.1101/gr.093310.109

Thakur, C., Qiu, Y., Fu, Y., Bi, Z., Zhang, W., Ji, H. and Chen, F., 2022. Epigenetics and environment in breast cancer: New paradigms for anti-cancer therapies. *Front. Oncol*., **12**. https://doi.org/10.3389/fonc.2022.971288

Vietri, M.T., D'Elia, G., Benincasa, G., Ferraro, G., Caliendo, G., Nicoletti, G.F. and Napoli, C., 2021. DNA methylation and breast cancer: A way forward (Review). *Int. J. Oncol*., **59**: 1–12. https://doi.org/10.3892/ijo.2021.5278

Vivarelli, S., Spatari, G., Costa, C., Giambò, F. and Fenga, C., 2024. Computational analyses reveal deregulated clock genes associated with breast cancer development in night shift workers. *Int. J. mol. Sci*., **25**: 8659. https://doi.org/10.3390/ijms25168659

Waters, K.M., Tan, R., Opresko, L.K., Quesenberry, R.D., Bandyopadhyay, S., Chrisler, W.B., Weber, T.J., 2009. Cellular dichotomy between anchorage-independent growth responses to bFGF and TPA reflects molecular switch in commitment to carcinogenesis. *Mol. Carcinog*., **48**: 1059–1069. https://doi.org/10.1002/mc.20558

Xiang, D., Gu, M., Liu, J., Dong, W., Yang, Z., Wang, K., Fu, J. and Wang, H., 2023. m6A RNA methylation-mediated upregulation of HLF promotes intrahepatic cholangiocarcinoma progression by regulating the FZD4/β-catenin signaling pathway. *Cancer Lett*., **560**: 216144. https://doi.org/10.1016/j.canlet.2023.216144

Xiang, D.-M., Sun, W., Zhou, T., Zhang, C., Cheng, Z., Li, S.-C., Jiang, W., Wang, R., Fu, G., Cui, X., Hou, G., Jin, G.-Z., Li, H., Hou, C., Liu, H., Wang, H. and Ding, J., 2019. Oncofetal HLF transactivates c-Jun to promote hepatocellular carcinoma development and sorafenib resistance. *Gut*, **68**: 1858–1871. https://doi.org/10.1136/gutjnl-2018-317440

Zhou, H. and Wang, F., 2023. Tensin 1 regulated by hepatic leukemia factor represses the progression of prostate cancer. *Mutagenesis*, **38**: 295–304. https://doi.org/10.1093/mutage/gead027